行政院國家科學委員會專題研究計畫　期中進度報告

以網路模型探討布朗膠體在過濾器中的過濾行為(1/3)

計畫類別：個別型計畫
計畫編號：NSC93-2214-E-029-003-
執行期間：93 年 08 月 01 日至 94 年 07 月 31 日
執行單位：東海大學化學工程學系

計畫主持人：張有義

報告類型：精簡報告
報告附件：出席國際會議研究心得報告及發表論文
處理方式：本計畫可公開查詢

中　華　民　國 94 年 5 月 10 日

期中精簡報告

以網路模型探討布朗膠體在過濾中的過濾行為(1/3)

NSC 93-2214-E-029-003

張有義教授

台中市東海大學化工系

Abstract

The effect of different interaction energy curves of DLVO theory on the permeability reduction in a filter bed is investigated by using the Brownian dynamics simulation method and the modified square network model to track the individual particles movement through the filter bed. When energy barrier exists and both particle and pore size distributions are of the Raleigh type, it is found that particles with Brownian motion behavior are easier to get straining at small pores, and cause higher permeability reduction than those without considering the Brownian motion behavior. But, this result was not observed for the constant particle and pore sizes case. The permeability reduction for the Raleigh size distribution is higher than that of the constant size. Similar results are also obtained for the "barrierless" type interaction energy curve for the case of Raleigh type size distribution, with the exception that the decreasing rate of permeability reduction of Brownian particles is smaller than that without considering the Brownian motion behavior.

Email:yichang@mail.thu.edu.tw Fax:00-886-4-23590009

1. Introduction

In order to describe the effect of pore size distribution on the particle deposition behavior along the filter bed properly, the network model has been applied extensively to simulate the formation of porous media since the pioneer work of Todd et al. (1984) twenty years ago. A review paper describing the continuum and discrete models of particle transport and gas reaction processes in disordered porous media was given by Sahimi et al. (1990), at which the statistical physics of disordered media was well described, and the topology of porous media can be defined by using the coordination number Z; for example, Z=4 stands for a simple square network model and $Z \rightarrow \infty$ stands for a parallel capillary tube network in a two-dimensional coordinate. Applying this coordination number and the conductance calculation method of the effective medium approximation (EMA) (Kirkpatrick, 1973), Sharma and Yortsos (1987) had successfully established a set of population balance equations, and calculated the temporal variations of the filter coefficient caused by the particle deposition in a filter bed. In their model, two types of particle deposition mechanisms, straining and direct deposition, were being considered in the capillary tube model. The permeability reductions resulting from particle's deposition were then calculated by using EMA, where the fluid velocity is assumed to be the same in all pore throats of a given size in the network. Then, applying the principle of flow biased probability and the concept of wave front movement, both Rege and Fogler (1988) and Imdakm and Sahimi (1991) predicted the permeability and the effluent concentration of particles, and were in good agreement with the available experimental data. Later on, by viewing the void space of porous media as a constricted tube unit bed element (UBE), Burganous et al. (1992) had developed a three-dimensional network simulator to calculate the filter coefficient, at which the deposition rate of particles is determined by using the method of trajectory analysis. But, in their force balanced equations, the Brownian diffusion force of particles was not considered.

In the present paper, with the adoption of the Brownian dynamic simulation method mentioned above, we used the two-dimensional modified square network model (see Fig. 1) to track the individual particles with Brownian motion behavior as they move through the filter bed. From which, caused either by the straining or by the direct deposition of

particles on the pore walls, the temporal variations of the permeability reduction and the pressure drop can be determined. The type of sinusoidal constricted tube (SCT) will be adopted in the present simulation. In addition, the effects of the total interaction energy curve of DLVO theory with various shapes (Verwey and Overbeek, 1948) are also investigated.

2. Theoretical formalism

In the present study, we use the modified two-dimensional square network (as shown in Fig. 1) to represent the porous media of the filter, and adopt the Brownian dynamic simulation method to track the individual particles as they move through the network. In Fig. 1, all bonds (i.e. pores) in the network are assumed to have the same length, but with a Raleigh form pore size distribution (Sharma and Yortosis, 1987):

$$f_p(r') = 2r'\exp(-r'^2) \qquad (1)$$

where f_p and r' are the dimensionless distribution density and the dimensionless radius of pores, respectively. Eq. (1) satisfies the following equation,

$$\int_0^\infty 2r'\exp(-r'^2)dr' = 1 \qquad (2)$$

This distribution can then be assigned randomly to the bonds in the network as follows,

$$\int_0^{r_1'} 2r'\exp(-r'^2)dr' = 1-\exp(-r_1'^2) \qquad (3)$$

with

$$r_1' = \frac{r_f}{r_{mean}} = \sqrt{-\ln(1-a_i)} \qquad (4)$$

and $0 < a_i < 1$

where the random number a_i can be generated by using the standard computer software (IMSL, 1985) and r_{mean} is the mean radius of pores. A typical diagram of Raleigh distribution is shown in Fig. 2. Eq. (4) can also be applied to determine the particle size distribution randomly in the computer simulations described as follows.

As particles of a given size distribution transport through a bond shown in Fig. 1, they will arrive at a node where the fluid will be separated by two paths to flow further into the network. In the present study, we adopt the method of flow biased probability to determine either one path for particles to flow through (Rege and Fogler, 1988). As shown in Fgi.1, when a particle encounters a node in the network, it has a choice of exit path. The exit path is selected randomly in the present model, but with a bias toward the paths with greater flow rates. Usually, the greater the flow rate, the greater the probability of the particle choosing that path. Details of this method can be found elsewhere (Rege, Ph.D. thesis, 1988).

In the current model, two different mechanisms of particle capture are considered: straining (size exclusion) and direct deposition. Straining occurs when the particle diameter is larger than the pore diameter selected for it to transport through the network. Straining plugs up the pore and drops its permeability to zero, and thereby changing the flow direction to other available pores. Direct deposition of a particle on a pore wall occurs as a result of hydrodynamic and DLVO interaction forces acting on the particle. Details of the Brownian dynamics simulation method can be found in my 2004 NSC report **(NSC 92-2214-E-029-002).**

3. Simulation results

The parameter values adopted in the simulation are: ε_{i0} = 0.4, r_f =10.0 μm, r_{pm} = 0.5 μm and C_{in} = 1000 particles per cm^3. Similar simulation procedure of tracking individual Brownian particles to move through the network described in our previous paper is adopted (Chang et al, 2004). Simulations are performed on a two-dimensional network with $N_L = 70x70$, and the influent flow rate is kept at constant.

The effects of the four types of interaction energy curves on the permeability ratio will be investigated in the present section. As shown in Fig. 2, curves A exhibits a large primary maximum and a deep secondary minimum; curve B displays a large primary maximum and a negligible secondary minimum; while curve C has a deep secondary minimum only and a

"barrierless" interaction energy curve is represented by curve D. In this figure, N_{E1}=105.0 and N_{DL}=10.75 for curve A, N_{E1}=50.0 and N_{DL}=5.02 for curve B, N_{E1}=77.0 and N_{DL}=10.0 for curve C, N_{E1}=0.0 and N_{DL}=0.0 for curve D, and N_{E2}=1.0 and N_{L0} =7.0 for all four curves. Our previous paper (2003) calculated the collection efficiencies of particles in SCT, and found that the collection efficiency of curve D is always greater than that of other three curves when Reynolds number of fluid is small because there is no energy barrier exists, and the deposition mechanism of particles is controlled by the Brownian diffusion effect. For curves A, B and C, it was found that, even with the presence of the deep secondary minimum which increases the accumulation probability of particles for curves B and C, the steepest slope between the secondary minimum and the primary maximum energy barriers of curve A is still the main reason for its lowest collection efficiency among these three curves. But, when Reynolds number becomes large, because of a greater sweep away probability caused by the tangential fluid convection force acting on those particles accumulating at the secondary minimum, the collection efficiency of curve C is smaller than that of curve B.

Corresponding to curve A in Fig. 2, the simulation results of the permeability ratio as the function of pore volumes injected are given in Fig. 3a. In this figure, the case that the particle and pore sizes are of the Raleigh distribution and the constant value case are considered with the Brownian diffusion effect included. For the case of Raleigh type distribution, both the large primary maximum of curve A and the Brownian diffusion effect are unfavorable for the particles to deposit on the pore walls, and particles with Brownian motion behavior can transport more particles into the network and increase the probability of straining small pores, consequently can cause a higher permeability reduction than that without considering Brownian diffusion effect. But, this result is not observed for the case when both the particle size and the pore size are fixed at a constant value. Also, because of the straining effect, the permeability ratio for the case of Raleigh distribution is always lower than the case of a constant size value. Between the distribution of pore size and of particle size, our simulation showed that the pore size distribution has bigger effect on reducing the permeability ratio than that of the particle size distribution. In the above simulations, we found that straining is the main mechanism to reduce the permeability at the initial period of injection for the case of Raleigh distribution, and vice versa for the case of constant size value where the direct deposition mechanism becomes dominant. This result can explain why the initial decreasing rate of K/K_0 for the case of Raleigh distribution is higher than that of the case of constant size value as shown in Fig. 3a. Corresponding to Fig. 3a, the simulation results of pressure drop are shown in Fig. 3b. Those particles with Brownian motion behavior and with a Raleigh size distribution own the highest pressure drop among these four cases investigated.

Corresponding to the “barrierless” curve D (which favors particle’s deposition), the relationships between the permeability ratio and the pore volumes injected are shown in Fig. 4a. Similar to results shown in Fig. 4a, the permeability ratio for the case of Raleigh distribution is lower than that of the case of a constant size value. The pore size distribution and the straining mechanism still dominate the reduction of the permeability at the initial period of filtration. But, for the case of Raleigh type distribution when the Brownian diffusion effect is considered, because those Brownian particles can spread wider over the bonds at the entrance region in the network, hence its decreasing rate of permeability ratio is smaller than the case without considering the Brownian diffusion effect as shown in Fig. 4a. Similar result is obtained for the case of constant size value. Corresponding to Fig. 4a, the pressure drop simulation results are shown in Fig. 4b. Among which, the case of Raleigh distribution without considering the Brownian diffusion effect gives the highest pressure drop.

For the case that both particle and pore sizes are of the Raleigh type distribution, and the Brownian diffusion effect is included, Fig. 5 summarizes the simulation results

of the permeability ratio K/K_0 versus pore volumes injected for these four different interaction energy curves shown in Fig. 2. As expected, the order of the magnitudes of K/K_0 in general is: curve D > curve C > curve B > curve A. Since there is no energy barrier exists, the mechanism of direct deposition becomes dominant in pores, hence the permeability ratio of curve D is always greater than that of the three other curves. Conversely, the permeability ratio of curve A is the lowest among the four curves because it has the steepest slope between the secondary minimum and the primary maximum, which causes more Brownian particles to block more of the small pores. The fact that the K/K_0 value of curve B is smaller than that of curve C implies that the height of the primary maximum plays a more important role in decreasing the deposition rate of particles than that of the depth of the secondary minimum.

4. Conclusion

The present simulation method can successfully predict the temporal permeability reduction by tracking the Brownian particles move through the filter bed. Our method also takes different size distributions of both particles and pores into account. The effects of the interaction energy curves of DLVO theory of various shapes were also investigated.

5. References:

1. Burganos, V. N., Paraskeva, C. A., & Payatakes, A. C. (1992). *J. Colloid Interface Sci.*, 148(1), 167-181.

2. Chang, Y. I., Chen, S. C., & Lee, E. (2003). *J. Colloid Interface Sci.*, 266(1), 48-59.

3. Chang, Y. I., Chen, S. C., Chan H. C. & Lee, E. (2004). *Chemical Engineering Science*, 59:4467-4479. (SCI).

4. Imdakm, A. O., & Sahimi, M. (1991). *Chemical Engineering Science*, 46(8), 1977-1993.

5. IMSL Libraries, IMSL (1985), Houston, Texas.

6. Kirkpatrick, S. (1973). *Rev. Mod. Phys.*, 45(4), 574-588.

7. Rege, S. D., & Fogler H. S. (1988). *A.I.Ch.E. J.*, 34(11), 1761-1772.

8. Sahimi, M., Gavalas, G. R., & Tsotsis, T. T. (1990). *Chemical Engineering Science*, 45(6), 1443-1502.

9. Sharma, M. M., & Yortsos, Y. C. (1987). *A.I.Ch.E. J.*, 33(10), 1644-1653.

10. Todd, A. C., Somerville, J. E., & Scott, G. (1984). *SPE*, No. 12498, Denver, Colorado.

11. Verwey, E. J. W., & Overbeek, J. Th. G. (1948). *Theory of the stability of lyophobic colloids*. Amsterdam: Elsevier.

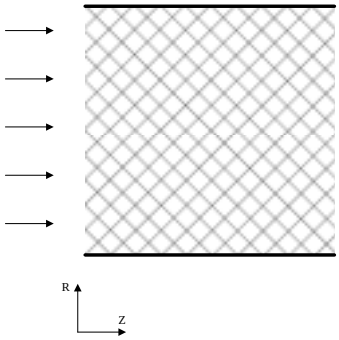

Figure 1. The simple modified square network model.

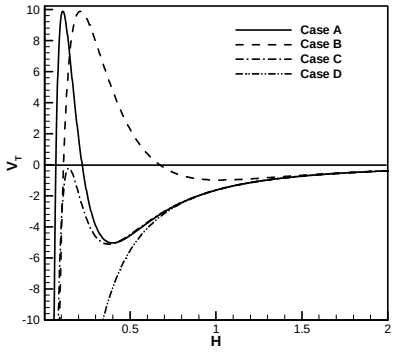

Figure 2. Four types of total interaction energy curves adopted in the simulation of the present paper.

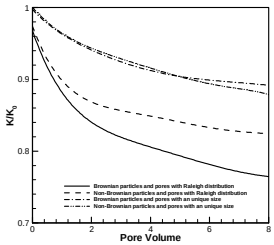

Figure 3(a). Effect of both particle and pore size distributions on the permeability ratio K/K_0 as the function of pore volumes injected, corresponding to curve A shown in Fig. 2.

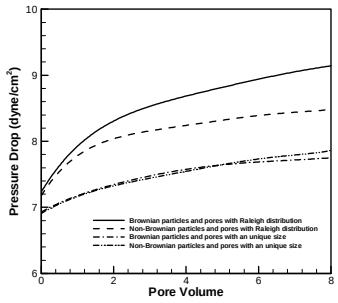

Fig. 3(b). The corresponded pressure drop obtained by using the present model..

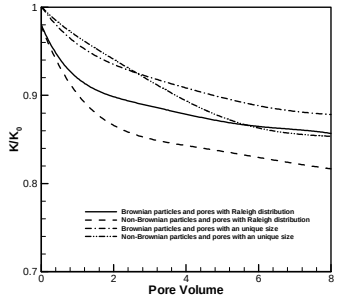

Figure 4. (a). Effect of both particle and pore size distributions on the permeability ratio K/K_0 as the function of pore volumes injected, corresponding to curve D shown in Fig. 2.

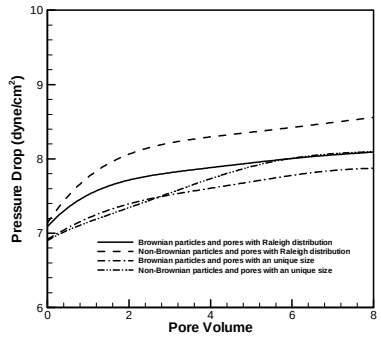

Fig. 4(b). The corresponded pressure drop obtained by using the present model..

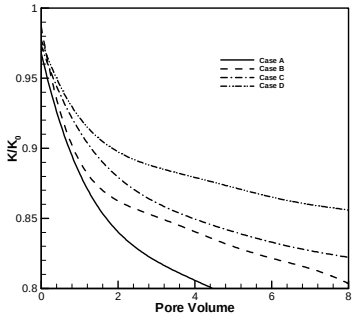

Figure 5. Effect of the four different interaction energy curves shown in Fig. 2 on the permeability ratio K/K_0 as the function of pore volumes injected, when both the particle size and the pore size are all with Raleigh type distribution form. on the permeability ratio K/K_0 as the function of pore volumes injected,